Finite Element Analysis of Stresses Due to Normal and Sliding Contact Conditions on an Elastic Surface

Authors:

Anantha Ram B.S., Joachim Danckert, Torben Faurholdt
Aalborg University, Denmark

Correspondence:

Anantha Ram B.S.
Department of Production, Aalborg University,
Aalborg, Denmark - 9220

Tel : +45 96 35 8958
Fax : +45 96 15 3030
Email: ananth@iprod.auc.dk

Keywords:
FEA, contact stresses, hard coatings

Notations:

$2a$	The contact zone or the contact width (μm)
a	Semi contact width (μm)
x	x distances along X-direction (μm)
y	y distances from the surface along the mirror axis in Y-direction (μm)
ν	Poisson's ratio of the workpiece (μm)
ν_i	Poisson's ratio of the indenter
E	Young's modulus of the workpiece (GPa)
E_i	Young's modulus of the indenter (GPa)
R	Effective radius (μm)
r	Radius of the workpiece (μm)
r_i	Radius of the indenter (μm)
E^*	Effective Young's modulus (GPa)
P_{max}	Maximum contact pressure (MPa)
$P(x)$	Pressure distribution (MPa)
F_n	Normal load per unit length in the Z-direction (N)
σ_x	Stress in the X-direction (MPa)
σ_y	Stress in the Y-direction (MPa)
σ_z	Stress in the Z-direction (MPa)
σ_{vm}	von Mises effective stress (MPa)
μ, fric	Co-efficient of friction

ABSTRACT

Wear prediction necessitates the investigation of elastic stresses developed in the workpiece material due to impact and sliding of abrasive particles in tribological contact situations. LS-Dyna implicit finite element analysis is used to investigate these contact stresses in the workpiece material under imposed Hertzian pressure loading. A line contact condition (cylindrical body on a plane surface) is assumed and the predicted stress field is compared with analytical solutions. The model is parametric, two-dimensional and built in LS-Ingrid in terms of semi contact width 'a'. Application of hertz pressure and implicit control cards are some of the issues of this study. The study is a preliminary step in the extension of the model where the workpiece will be modeled with a thin hard layer/coating under the same contact situations. It is found that the finite element model developed, predicts the elastic stresses in close agreement with the theoretical results and the model can be suitably extended for analyzing contact situations of layered systems.

INTRODUCTION

Abrasive wear occurs when hard abrasive particles either slide across a surface or are trapped between two surfaces. Wear of a tool material is mainly influenced by the contact pressures and friction induced by these abrasive particles (such as Al_2O_3, SiO_2) [1]. The harder the surface compared to the abrasive particles, lesser the wear is to be expected. Usually metal surfaces of tools and machine elements are softer than the particles they come into contact during their service life which leads to their severe wear. It is possible to reduce wear by appropriate surface treatment such as hard protective coatings like Titanium Nitride (TiN), Titanium Carbide (TiC) and Chromium Nitride (CrN). The size and

shape of the wear particle in contact does have an influence on the stresses it induces in the tool. Usually in practical applications, a 10 to 100 μm radius abrasive particles are common and such a tribological contact situation is assumed in the present study.

The abrasive particle is assumed to be cylindrical of radius 'r_i' and elastic. The workpiece (tool material) in contact is also considered as an elastic material and flat in nature of radius 'r'=∞. Figure 1 shows a two dimensional contact situation between an abrasive particle and a workpiece. Such a type of contact situation is usually referred as "Hertzian contact" [2][3]. The elastic contact creates a contact width of '$2a$' and the resulting elliptical pressure distribution on the workpiece material is known as "Hertzian pressure distribution". Due to the Hertzian pressure distribution, a stress field is created in the workpiece and if the von Mises stress developed reaches the yield strength of the workpiece, it starts to yield and wearing takes place. A finite element model is necessary to predict the elastic

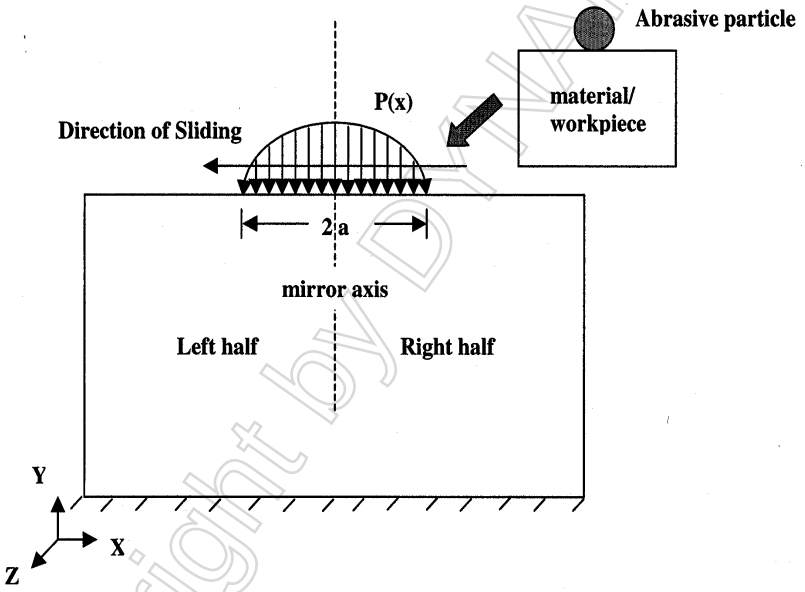

Figure 1: Schematic of an elastic contact (abrasive particle on a workpiece) and Hertzian pressure loading with sliding conditions.

stress field under such a contact to avoid the cumbersome theoretical calculations. The third dimension (Z-direction, see figure 1) is assumed to be infinite and hence plane strain conditions is applied in the modeling. The present work is to model only the workpiece or tool material subjected to such a tribological contact situation and later on extend the same model by building a thin hard layer/coating onto it. Such an investigation helps in understanding the load bearing capacity of coating-substrate systems when compared to the uncoated one and may help in selection of coatings.

Hertz presented the original solutions in 1881 and his formulations[1] were [2],

$$a^2 = \frac{4F_n R}{\pi E^*} \tag{1}$$

where, 'a' is the resulting semi contact width. In equation 1, 'E^*', the effective elastic modulus and 'R', the effective radius are given by equations 2 and 3 respectively.

$$\frac{1}{E^*} = \left[\frac{1-\nu^2}{E} + \frac{1-\nu_i^2}{E_i}\right] \tag{2}$$

$$\frac{1}{R} = \frac{1}{r} + \frac{1}{r_i} \tag{3}$$

The resulting contact zone/width, 'a' as shown in figure 1, will be under an elliptical pressure distribution as shown in equation 4 where 'P_{max}', the maximum contact pressure is given by equation 5. In the figure, the sliding condition is shown by an arrow indicating the direction of sliding. The sliding condition is approximated as, at some time frame both normal and tangential load (frictional load) acts simultaneously. Friction at the surface has an influence on the elastic stress field [4] and the present study involves the influence of friction on the elastic stress field.

$$\frac{P(x)}{P_{max}} = \left[1 - \left(\frac{x}{a}\right)^2\right]^{1/2} \tag{4}$$

$$P_{max} = \frac{2F_n}{\pi a} \tag{5}$$

There are two basic approaches in modeling of contact situations. In the first approach, an elastic plane surface is assumed to be loaded by an elastic indenter (say an abrasive particle) so that the surface displacements can be prescribed and the resulting stress field can be computed. In the second approach the indenter is not modeled and the elastic plane surface is simply subjected to a known pressure distribution [5][6] that created by an indenter of known size and properties. In a recent work by Subutay et al [7] using LS-Dyna FE-solver, they have modeled by the first approach and their results predicted are 10-15% higher to the theoretical stress field. Mass scaling, mesh convergence and explicit integration method are some of the highlights of their study. In our study the second approach is chosen as the loading condition, the simulations are carried out implicitly and the results are compared to the theoretical solutions. The advantages of the second approach are discussed at the end.

Under plane strain condition the explicit equations of stresses (principal stresses) for the above defined contact conditions under both under normal loading and tangential tractions were given by Djabella et al [5] and Smith and Liu [8]. According to directions shown in figure 1,

Below the contact zone and along the mirror axis in Y-direction the stress 'σ_x' is given by equation 6,

$$\frac{\sigma_x}{P_{max}} = -\frac{1}{a}\left[\frac{a^2 + 2y^2}{(a^2+y^2)^{1/2}} - 2y\right] \tag{6}$$

[1] those notations which are not specifi ed in the text under certain equations should be read from the fi rst page

the stress 'σ_y' along the mirror axis in Y-direction is given by equation 7,

$$\frac{\sigma_y}{P_{max}} = -\frac{a}{(a^2+y^2)^{1/2}} \tag{7}$$

and the stress 'σ_z' along the mirror axis in Y-direction is given by equation 8,

$$\frac{\sigma_z}{P_{max}} = -\frac{\nu}{P_{max}}(\sigma_x + \sigma_y) \tag{8}$$

At the surface, within the contact zone/width, the stresses 'σ_x' and 'σ_y' are given by equation 9 and stress 'σ_z' is given by 10.

$$\frac{\sigma_x}{P_{max}} = \frac{\sigma_y}{P_{max}} = \frac{P(x)}{P_{max}} = -\left[1-\left(\frac{x}{a}\right)^2\right]^{1/2} \tag{9}$$

$$\frac{\sigma_z}{P_{max}} = -2\nu\frac{P(x)}{P_{max}} \tag{10}$$

According to the Hertz theory, in the above described elastic contact situations, the maximum shear stress lies at $0.78a$ beneath the surface (along mirror axis in the Y-direction) and has a magnitude of $0.31P_{max}$. The effect of friction is to add compressive stress near one edge of the contact and to intensity the tensile stress at the other edge of contact zone depending upon the direction of sliding. Friction also increases the von Mises effective stress (σ_{vm}) in the workpiece material. As friction increases, 'σ_{vm}' also increases and lies closer to the surface. Above a value of 0.3, 'σ_{vm}' lies on the surface according to theory [4] and wearing is more pronounced.

Smith and Liu [8] have given the stress distributions in the contact zone at the surface when co-efficient of friction, 'μ'=0.3333 in their work. The stress 'σ_x' is given by equation 11 and stress 'σ_z' is given by 12.

$$\frac{\sigma_x}{P_{max}} = -\left[\sqrt{1-\frac{x^2}{a^2}} + \frac{2}{3}\frac{x}{a}\right] \tag{11}$$

$$\frac{\sigma_z}{P_{max}} = -\nu\left[2\sqrt{1-\frac{x^2}{a^2}} + \frac{2}{3}\frac{x}{a}\right] \tag{12}$$

The theoretical predictions of stresses in presence of a coating in similar contact situations can be very complicated and Finite Element Method (FEM) is definitely a easier and a faster way to predict the same. The main idea of this paper is to compare the finite element predicted stresses with the theoretical ones presented above for the workpiece alone. The modeling method and the loading is a verification step in order to use the same model for predicting the stresses in layered systems.

FINITE ELEMENT ANALYSIS (FEA) AND APPROACH

Figure 2 shows a full finite element model. The model is built in LS-Ingrid [9] using normal and magic parts in terms of semi-contact width[2] 'a'. The semi-contact width 'a', has 160

[2] $a = 4\mu$m

elements such that the left half is a mirror of the right half along the mirror axis as shown in the figure. In total 46054 nodes and 42444 elements constitute the finite element model. Plane strain shell element formulation and fully integrated elements are used for the analysis. Elastic properties of that of steel (E=210 GPa, ν=0.3) are used. All the nodes in the bottom are constrained from motion and translation. Some studies [10][11] have shown that the half model dimensions of $\approx 20a$ would predict the correct stress field and hence the model dimensions are $40a$ in X and $20a$ Y-direction. In practice, the pressure distribution is transformed into "Equivalent or Resulting Nodal Force, R_n" where $n = 1, 2, 3, ...161$, is the number of nodes starting from the mirror axis. The top part of the figure 2 shows the transformation of normal pressure in addition with frictional loads to resultant nodal force for the first plane element "E_1" of size "e". At first the normal pressure "P_1" on the element "E_1" is transformed to equivalent nodal force "W_1"on both the nodes "N_1" and "N_2" as

$$W_1 = \frac{P_1 e}{2} \tag{13}$$

If a frictional traction load "f_1" is assumed to act on the element "E_1" at nodes "N_1" and "N_2" approximating sliding conditions, then $f_1 = \mu W_1$ where 'μ' is the co-efficient of friction. Such a combination of loading (normal+frictional load) is transformed into a "Resultant Nodal Force, R_1" acting on nodes "N_1" and "N_2" as

$$R_1 = \sqrt{W_1^2 + f_1^2} \tag{14}$$

such that it acts in a direction which simulates the combined loading. For successive elements, "E_2, E_3,.....E_{160}" on both the halves which share a common node with their preceding element, the resultant nodal forces are added correspondingly. Thus for the successive nodes "N_2, N_3, N_4.....N_{161}" on both halves, "$(R_1 + R_2)$, $(R_2 + R_3)$, $(R_3 + R_4)$.....$(R_{160} + R_{161})$" will be the resultant nodal force respectively. On the node "N_1", the resultant force will be "$2R_1$" since it is the common node separating the two halves. A new co-ordinate system is defined according to the desired co-efficient of friction 'μ' and the direction of action of the resultant force on the each node is specified by it (see magnified view of top surface elements in figure 2). When μ = 0, the analysis corresponds to only normal loading. When $0 < \mu \leq 1$, frictional load also acts in combination with the normal loading to approximate sliding conditions of an abrasive particle on a workpiece.

The resultant nodal forces on nodes "N_1, N_2, N_3, N_4.....N_{161}" are applied by nodal point forces through a loadcurve. The loadcurve is scaled accordingly which corresponds to the magnitude on each node viz., $(2R_1)$, $(R_1 + R_2)$, $(R_2 + R_3)$, $(R_3 + R_4)$.....$(R_{160} + R_{161})$. The point forces on each node is built-up using Fortran and Unix shell programming. The loadcurve is ramped to the maximum value in 20 secs and held constant till 25 secs with a time step of 1 sec. Implicit control cards are used to run the simulation implicitly [12].

RESULTS

After the simulation the stresses are picked out from the surface elements along X-direction and the elements along the mirror axis in Y-direction (see fig 2) using LS-Post [13]. For easier data collection, Fortran programs assisted the handling and displaying of the results. The stresses are normalized with respect to the maximum contact pressure[3] 'P_{max}' and the

[3] P_{max}=1500 MPa

spatial distances along X and Y-directions are normalized with respect to the semi-contact width 'a'.

- As a result of the resultant nodal forces making up the applied pressure distribution, figure 3 shows the applied FEM Hertz pressure distribution which follows very closely with the theoretical pressure distribution as per equations 4 and 5.
- Figure 4 shows the computed normalized stress (σ_x) in the subsurface along the mirror axis (Y-direction) by FEM and that given by theory as per equation 6.
- Figure 5 shows the computed normalized stress (σ_y) in the subsurface along the mirror axis (Y-direction) by FEM and that given by theory as per equation 7.
- Figure 6 shows the computed normalized stress (σ_z) in the subsurface along the mirror axis (Y-direction) by FEM and that given by theory as per equation 8.
- Figure 7 shows the comparison of computed normalized stress (σ_x) with the theoretical stresses in the surface within the contact width '$2a$' (X-direction). The results are computed for both with (μ=0.3333) and without friction (μ=0). The theoretical stress for both with (μ=0.3333) and without friction follows as per equations 11 and 9 respectively.
- Figure 8 shows the comparison of computed normalized stress (σ_z) with the theoretical stresses in the surface within the contact width '$2a$' (X-direction). The results are computed for both with (μ=0.3333) and without friction (μ=0). The theoretical stress for both with (μ=0.3333) and without friction follows as per equations 12 and 10 respectively.
- Table 1 shows some additional results. The theoretical results are calculated assuming a Al_2O_3 abrasive particle of radius 'r_i'=50 μm, 'E_i'=400 GPa, 'ν_i'=0.2, 'P_{max}' = 1500 MPa and the properties of the workpiece are as that of High Speed Steel - HSS (E=210 GPa, ν=0.3). According to theory, the maximum shear stress = $0.31P_{max}$ and occurs at a distance of $0.78a$ from the surface along the mirror axis (Y-direction).
- If the HSS tool steel is assumed to fail when the effective von Mises stress (σ_{vm}) reaches its yield strength (σ_{yield}=1950 MPa [14]), then the steel under the above said contact conditions can sustain a maximum pressure of $\approx$ 3400 MPa before yielding initiates. It is seen from the simulations that the von Mises stress reaches the yield quickly when the frictional traction is increased and the load bearing capacity decreases in conformation with theory [4]. Figure 9 shows the computed normalized stress (σ_{vm}) in the subsurface along the mirror axis (Y-direction) at μ=0 and μ=0.3333. It shows that when friction is more than 0.3, 'σ_{vm}' also increases and the maximum value almost lies in the surface.

CONCLUSIONS

The obtained/predicted results by finite element analysis using the above finite element model is in very good agreement with the theoretical results. This model can be suitably extended to the computation of stresses in layered systems employing the same loading conditions and thus finding out the load bearing capacity between coated and uncoated systems. The error between the computed results and the theoretical results is $< 2.5\%$

Table 1: Additional Results

	Theory	Computed Results
Maximum shear stress (MPa)	465	474.86
Depth of maximum shear stress from the surface along the mirror axis in Y-direction (μm)	3.12	3.10

when compared to 10-15% error reported in the earlier works [7]. Moreover, since the simulation is carried out implicitly without any contact algorithm, the simulation is much faster. Many simulations can be carried out with layered systems to have a wide range of results within less time.

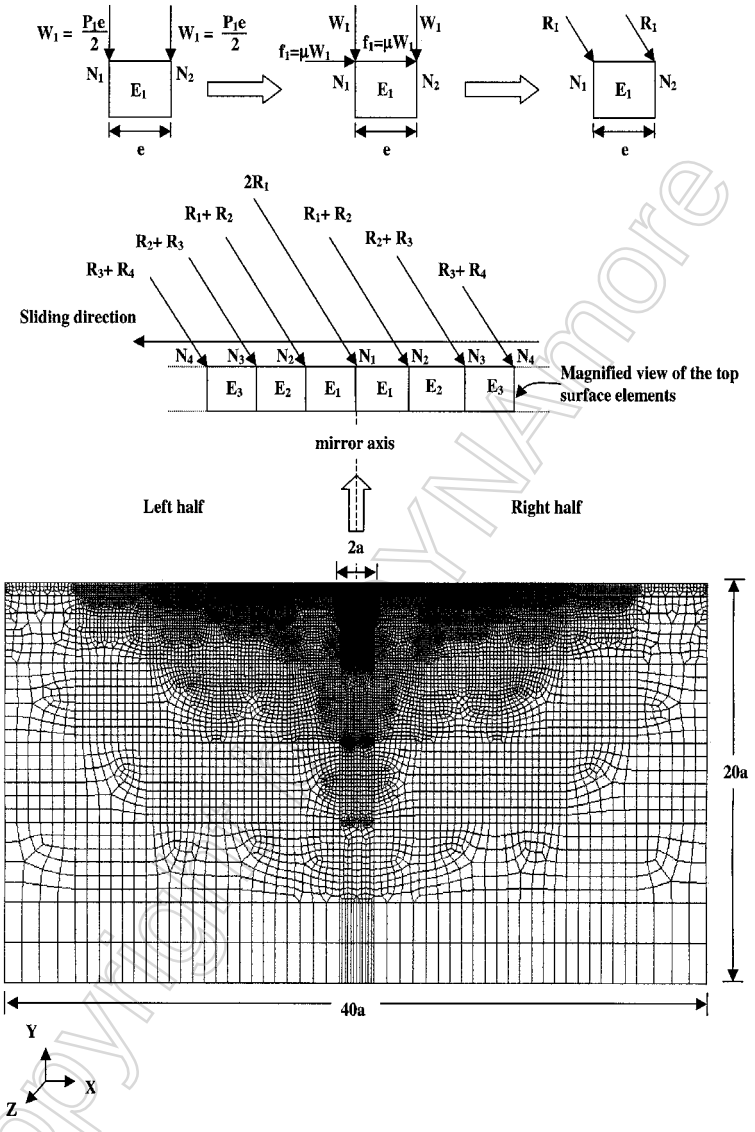

Figure 2: Finite element model with details of applied normal and frictional loads to simulate normal loading and sliding conditions.

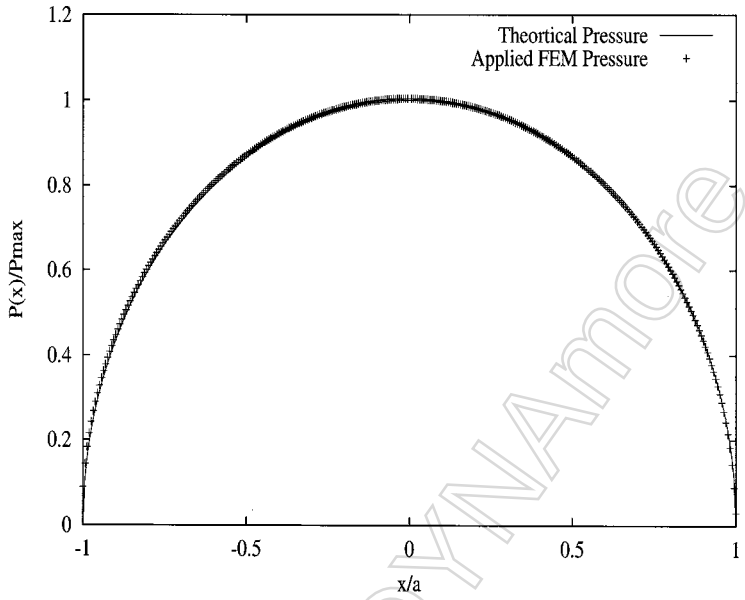

Figure 3: Applied normalized Hertzian pressure [$P(x)$ P_{max}] in the contact zone/width '$2a$' - in comparison with theory.

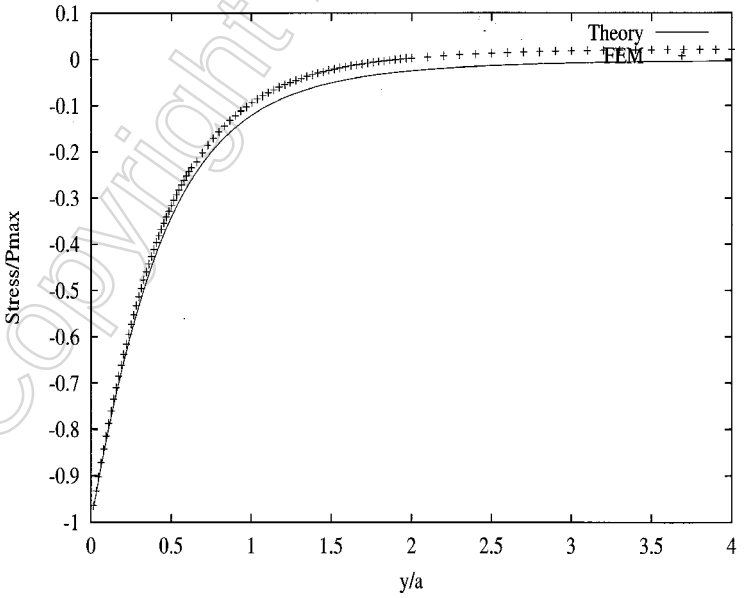

Figure 4: Normalized subsurface stress along the mirror axis (Y-direction) - σ_x/P_{max}

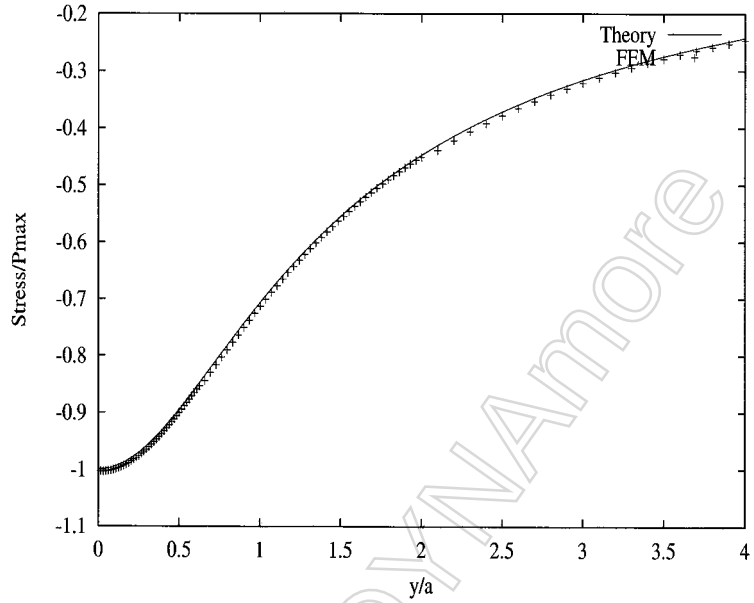

Figure 5: Normalized subsurface stress along the mirror axis (Y-direction) - σ_y / P_{max}

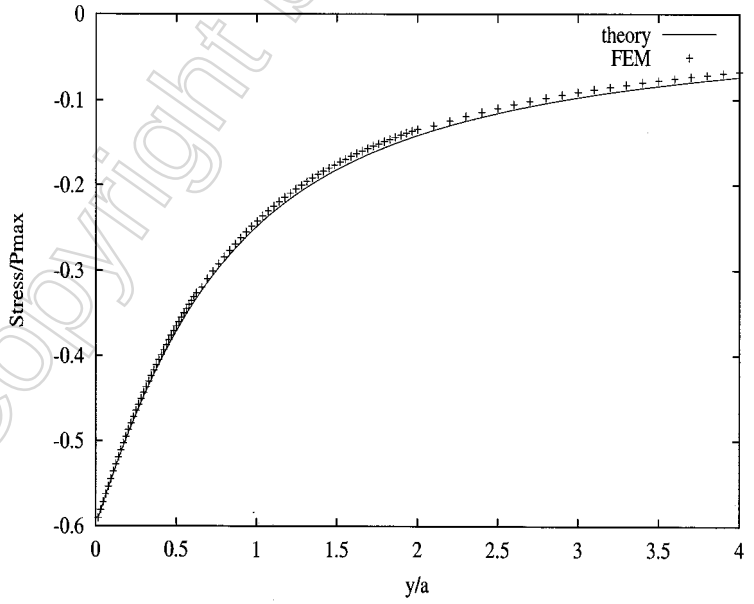

Figure 6: Normalized subsurface stress along the mirror axis (Y-direction) - σ_z / P_{max}

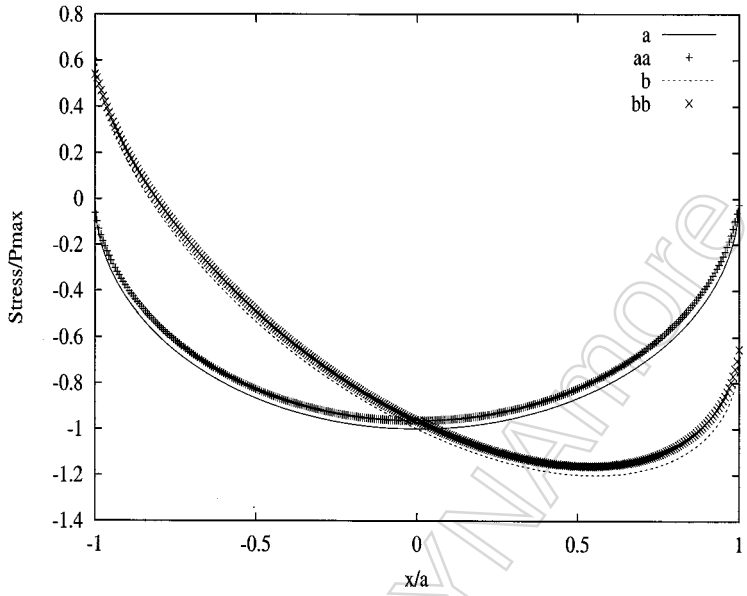

Figure 7: Normalized stress - 'σ_x/P_{max}', with and without friction. In the figure "a" represents theoretical stresses and "aa" represents FEM computed stresses at μ=0. "b" represents theoretical stresses and "bb" represents FEM computed stresses at μ=0.3333.

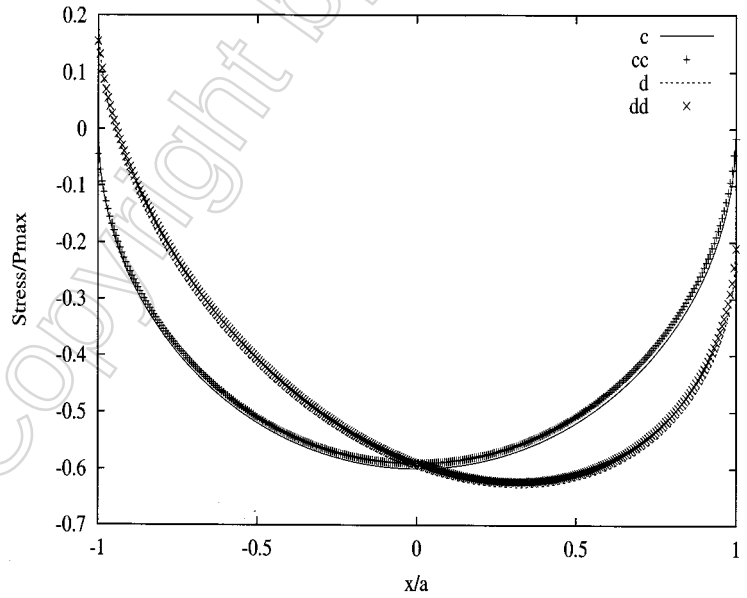

Figure 8: Normalized stress - 'σ_z/P_{max}', with and without friction. In the figure "c" represents theoretical stresses and "cc" represents FEM computed stresses at μ=0. "d" represents theoretical stresses and "dd" represents FEM computed stresses at μ=0.3333.

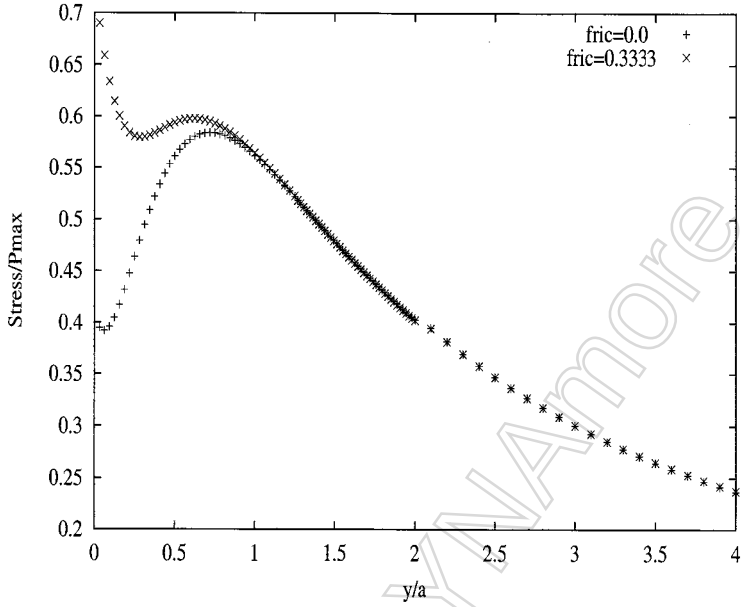

Figure 9: Computed normalized subsurface stress - 'σ_{vm}/P_{max}' at μ=0 and μ=0.3333. As friction increases it is seen that the effective stresses also increases and maximum value almost lies in the surface.

References

[1] KLOCKE F., SWEENEY K., and RAEDT H.W. (2001) “Improved tool design for fine blanking through the application of numerical modeling techniques”, Journal of Materials Processing Technology. Vol. 115, pp. 70-75.

[2] JOHNSON K.L. (1985) “Contact Mechanics”, Cambridge University Press, Cambridge England.

[3] HALLING J. (1975) “Principles of Tribology”, The Macmillan Press Ltd.

[4] KENNETH HOLMBERG and ALAN MATTHEWS. (1994) “Coatings Tribology”, Tribology Series 28, Elsevier publications.

[5] DJABELLA H. and KLAGES C.P. (1992) “Finite element analysis of contact stresses in an elastic coating on a elastic substrate”, Thin Solid Films. Vol 213, pp. 205-219.

[6] HOUMID BENNANI H. and TAKADOUM J. (1999) “Finite element model of elastic stresses in thin coatings submitted to applied forces”, Surface Coatings and Technology. Vol. 111, pp. 80-85.

[7] SUBUTAY AKARCA, WILLIAM J.A., and AHMED T ALPAS. (2002) “Finite element analysis between circular asperity and an elastic surface under plane strain condition”, 7^{th} International LS-Dyna User’s Conference.

[8] SMITH J.O and CHANG KENG LIU. (1953) “Stresses due to tangential and normal loads on an elastic solid with application to some contact stress problems”, Journal of Applied Mechanics.

[9] LS-INGRID (1998): “A pre-processor and three dimensional mesh generator for the programs LS-DYNA, LS-NIKE3D and TOPAZ3D vs 3.5”, LSTC, Livermore, USA.

[10] KOMVOPOULOS K. (1989) “Elastic-plastic finite element analysis of indented layered media”, ASME Journal of Tribology. Vol. 111, pp. 430-439.

[11] STEPHENS L.S., YAN LIU, and MELETIS E.I. (2000) “Finite element analysis of the initial yielding behaviour of a hard coating/substrate system with functionally graded interface under indentation and friction”, Journal of Tribology. Vol. 122, pp. 381-387.

[12] HALLQUIST J.O., LIN T., and TSAY C.S. (2001) “LS-DYNA vs. 960 Users Manual”, ”Nonlinear dynamic analysis of solids in three dimensions”, LSTC, Livermore, USA.

[13] LS-POST (1999): “A post-processor vs. 1.0”, LSTC, Livermore, USA.

[14] ANANTHA RAM B.S., JOACHIM DANCKERT, and TORBEN FAURHOLDT. (2003) “Break down of TiN coating on HSS steel substrates through rockwell indentation and inverse modeling of substrate behaviour”, A report, Department of Production, Aalborg University, Denmark.